Innovative Systems Design and Engineering
ISSN 2222-1727 (Paper) ISSN 2222-2871 (Online)
Vol.4, No.15, 2013
www.iiste.org

MPPT Based on Power Mapping and Frequency Derivative

Gaber El-Saady[1*] El-Nobi A. Ibrahim[1,2] Mahmoud Gelany[1,3]

1. Electric Engineering Department, Assiut University, Assiut, Egypt

2. Electric Engineering Department, Assiut University, Assiut, Egypt

3. Electric Engineering Department, Assiut University, Assiut, Egypt

* gaber1@yahoo.com

Abstract

This article presents a method for harmonic mitigation and maximum power point tracking for a variable-speed grid-connected wind turbine. The wind energy conversion system consists of a permanent magnet synchronous generator driven by variable-speed wind turbine. The output of the permanent magnet synchronous generator is connected to a single-switch three-phase boost rectifier to generate DC voltage, which feeds a current-controlled inverter to interface the system with the electric utility. The single-switch three-phase boost rectifier is an active power factor correction technique to maintain the power factor at the permanent magnet synchronous generator side to nearly unity and mitigate the permanent magnet
synchronous generator current harmonics. To mitigate inverter output current and voltage harmonics, an LCL filter has been used. Acomplete analysis of the harmonic content has been done everywhere in the system. The results show that the proposed maximum power point tracking control strategy succeeded to track the maximum wind power irrespective of the wind speed. This strategy in presence of an LCL filter achieved harmonic mitigation at the permanent magnet synchronous generator and inverter output sides.

Keywords: variable-speed wind turbine ; permanent magnet synchronous generator ; maximum power point tracking ; harmonic mitigation ; active power filter.

1. Introduction

Due to increased environmental concerns, electrical power generation from renewable energy sources (such as wind) is increasing. A wind energy conversion system (WECS) is suitable for either grid integration or as a stand-alone system used for the electrification of remote areas [1]. The rotating speed of the wind turbine is usually slow. Therefore,wind turbine drives an induction generator through a gearbox at a speed around the synchronous speed for normal operation and good efficiency [2]. However, the gearbox adds to the weight, generates noise, demands regular maintenance, and increases losses.The maintenance of the gearbox-generator system may be difficult, because the nacelle is located at the top of the tower. Furthermore, there may also be problems with materials,lubrication, and bearing seals. A low-speed permanent magnet synchronous generator (PMSG) can be connected directly to the wind turbine, which results in a simple mechanical system. Many disadvantages can also be avoided in a gearless wind turbine generator. The noise caused mainly by a high rotational speed can be reduced. Also, high overall efficiency and reliability, reduced weight, and diminished need for maintenance are achieved. In the variable-speed operation, there is a reduction of the drive train, reduction in mechanical stresses, and increased energy capture [2, 3]. Using a variable-speed WECS, the maximum power from the turbine is achieved when the rotor speed follows the variation of wind speed in order to maintain the maximum aerodynamic efficiency of the turbine.During recent years, many different maximum power point tracking (MPPT)control strategies have been developed [4–13]. A review of recent publications shows that there is very little agreement on the gain in projected energy [14]. In [4], the MPPT control strategy is based on the signal available from an anemometer. Other control strategies use mechanical sensors to measure the rotor speed [5–10]. The disadvantage of using an anemometer is the inaccuracy of the MPPT control strategy being based on the anemometer accuracy. The time response of the anemometer is also large compared to the electrical systems response. Also, the use of mechanical sensors to measure the rotor speed has the same disadvantages. Others [11, 12] used sensorless MPPT control,but the control algorithm is complicated. All previous reports [4–12] studied MPPT without paying attention to the harmonic contents in the WECS. In [13], a three-phase uncontrolled rectifier was used for conversion from AC to DC, and the MPPT algorithm was applied for controlling the inverter switching without paying attention to the harmonic contents. In this article, the modeling and simulation of a variable-speed grid-connected 20-kW wind turbine are implemented using the PSIM software package with a proposed MPPT strategy. This strategy is based on the so-called “power mapping and frequency derivative” [13].

2. WECS Model

The block diagram of the proposed WECS is shown in Figure 1, where the system consists of a PMSG driven by a variable-speed 20-kW wind turbine, an AC-DC single switch three-phase boost rectifier, and a current-controlled inverter (CCI) to interface the system with the electric utility. Ii1, Ii2, and Ii3 are the PMSG output currents; Idc and Vdc are the rectifier output current and voltage. A brief description of each element of the system is given below.

2.1 Wind Turbine

The output mechanical power of the wind turbine is given [1] by the usual cube law equation (Eq. (1)):

$$Pm = 0.5CpAUw^3 \quad (1)$$

The tip speed ratio λ is expressed as :

$$\lambda = R\omega m / Uw \quad (2)$$

where [1]
Cp is the power coefficient, which is a function of tip speed ratio λ and blade angle β ;
A is the wind turbine rotor swept area (m^2) ;
Uw is the wind speed (m/s);
ρ is the air density ([kg/m^3]);
R is the radius of the rotor (m);
ωm is the mechanical angular velocity of the generator (r/sec).

The relationship in Eq. (2) is usually provided by the turbine manufacturer in the form of a set of non-dimensional curves. The Cp curve for the wind turbine used in this study
at β =0 is shown in Figure 2.
If the rotor speed is adjusted according to the wind speed variation, then one can extract maximum power from the turbine by fixing the power coefficient at its maximum
value (= 0.45) [1].

2.2 PMSG Model

Theoretical models for generator producing power from a wind turbine have been developed [15].

$$\upsilon q = -Riq + Lq(d\, iq/dt) - \omega eLdid + \omega e\lambda m \quad (3)$$

$$\upsilon d = -Rid + Ld(d\, id/dt) + \omega eLqiq \quad (4)$$

where
R and L are the machine resistance and inductance per phase,
υd and υq are the two-axis machine voltages,
id and iq are the two-axis machine currents,
λm is the amplitude of the flux linkages established by the permanent magnet, and
ωe is the angular frequency of the stator voltage.

The expression for the rotor electromagnetic torque is written [15] as follows:

$$Te = 1.5(p/2)[(Ld-Lq)iqid - \lambda miq]. \quad (5)$$

The relationship between ωe and ωm is expressed as :

$$\omega e = (p/2)\, \omega m \quad (6)$$

where p is the number of the PMSG poles.

2.3 Rectifier and CCI

As the wind speed is varying so the PMSG produces variable-voltage and variable frequency output. A single switch three phase boost rectifier is used to convert the PMSG output AC voltage to DC voltage [16]. The output DC voltage Vdc feeds a CCI. The CCI is capable of operation over a wide range of DC voltage. The performance and the effectiveness

of the inverter are enhanced by the use of the ramptime current control technique[17–20] to control the inverter. Figure 1 shows the complete ramptime current control inverter and the switching signal generation. All details of ramptime implementation were reported before [18, 19]. This current-control technique was used before for an active power filter (APF) [21] applied for harmonic mitigation in a DC load fed by a diode bridge rectifier. In practice, the IGBT switches are not ideal, so they do not turn on or off instantaneously. Therefore, it is necessary to include a dead time, as shown in Figure 3, to avoid ashort circuit that may happen when switches in the same leg of the IGBT bridge conduct simultaneously. This dead time is included in the control signals. For two switches in the same leg, the switch that is "on" is turned "off". Then, there is a fixed time delay (dead time) to allow the turn-off process to be completed successfully. After the dead time, the opposite switch is turned "on" as shown in Figure 3.

3. Proposed MPPT Control Strategy

The power generated from the wind turbine depends on the power coefficient Cp value.In order to maximize the output power from the turbine, the wind turbine should operate
at the maximum value of the power coefficient Cp (= 0.45).
For each wind speed in the range 6–12 m/sec, there is a value of the DC voltage Vdc, which achieves the maximum extracted power from the turbine (Figure 4). In order to extract the maximum power from the wind turbine generator (WTG) at a given wind speed, the generated DC voltage Vdc must closely match the maximum power dotted curve shown in Figure 4.
In order to construct the MPPT control strategy, a single-switch three-phase boost rectifier is used (Figure 1). The single-switch three-phase boost rectifier consists of an
input filter, a boost inductor, a three-phase diode rectifier, a switch Qb, and a DC-link filter capacitor Cf . When the switch Qb turns on, all three input AC phases become shorted through inductors Lia, Lib, and Lic . The three currents Iia, Iib , and Iic begin to increase at a rate proportional to the values of their phase voltages. When Qb turns off, diode Db becomes forward-biased, and the inductors discharge their stored energies to the DC link capacitor Cf .
The resistances Rs1 = Rs2 = Rs3 represent the PMSG resistance in addition to the line resistance. Also, the inductors Li1 = Li2 = Li3 represent the PMSG equivalent inductance in addition to the line inductance. Using the design methodology proposed by Prasad et al. [16], it is possible to determine the passive element values Lia(= Lib = Lic) and C1(= C2 = C3).
The PMSG-generated power is expressed as:

$$P = \frac{\omega_e k}{R_a + j x_s}\left(k_1 \omega_e - \frac{\pi}{\sqrt{6}} V_{dc}\right). \qquad (7)$$

Equation (7) shows that the power extracted from the wind turbine depends on the DC voltage Vdc and the output frequency ωe. There are optimal values of Vdc and ωe , which result in extracting maximum power from the wind turbine. Both the DC voltage and the output frequency are considered in the proposed MPPT, as they determine the output power from the turbine. The derivative of the stator frequency will make the system highly sensitive. The look-up table contains the maximum power curve in tabular form.The input to the look-up table is the calculated power by the controller, and the output is the reference DC voltage. The reference DC voltage is compared with the actual DC voltage, and the output of the comparison is fed to the proportional integrator (PI)controller. The output of the PI controller is compared with a voltage of triangular waveform in order to generate the switching pulses of the switch Qb. In order to evaluate the proposed MPPT, a comparison with previous control strategies was done [4, 22]. The proposed MPPT was compared with "MPPT using
anemometer"[4] and MPPT using a "fixed-voltage scheme" [22]. MPPT with anemometer is based on the PI controller being designed to derive the maximum possible power from the wind, irrespective of the wind speed. For the fixed-voltage scheme, the output voltage of the rectifier is fixed at a certain value. This value would typically be optimized, knowing

the Weibull distribution for wind speed at the site.The single-switch three-phase boost rectifier is used in the present work for harmonic mitigation at the PMSG side and compared with the use of the APF [21] (Figure 5).The APF is mainly designed to mitigate the current harmonics [21], which operates at 50 Hz frequency. A variable frequency synchronizer is designed based on a simple PI closed-loop system and introduced into the system to accommodate variable-frequency operation. The variable-frequency synchronizer consists of a second-order low-pass filter and a phase-locked loop (PLL) [23]. The low-pass filter will filter the generator output voltage signals before reaching the PLL. The purpose of the PLL [23] is to lock onto the phase shift and frequency of the input signal, thus providing a current reference signal to the APF.

4. LCL Filter and Harmonic Mitigation at Inverter Output Side

In order to eliminate the current and voltage harmonics in the inverter output side, an LCL filter has been used [24]. Figure1 shows the complete scheme diagram of an LCL filter connected between the CCI and the grid. The design of the LCL filter parametersis given step by step in detail in [24]. is given step by step in detail in [24].

5. Simulation Results

The WECS based on the proposed MPPT control strategy is shown in Figure 1. All results are obtained using the PSIM software package. A comparison between different MPPT

strategies and the proposed system has been done first. Figure6 shows a simulated wind profile and the corresponding generated power with the proposed MPPT and other MPPT
strategies. It is quite clear that the generated power by the proposed MPPT is higher than that generated by the fixed voltage strategy [22] but less than the power generated by MPPT with an anemometer [4]. The proposed MPPT has advantages over MPPT with an anemometer, as it does not use a mechanical sensor or anemometer. Therefore, it is simple in construction and easy in implementation for industrial applications. Figure 7 shows a second wind speed profile adopted in this simulation. The simulation results dictate that the control system succeeded in tracking the maximum power available from the wind turbine (Figure 7), where the power coefficient is kept mostly at its maximum value (= 0.45), as shown in Figure 8. It is quite clear that the DC voltage output follows the reference DC voltage to track the maximum power, as shown in Figure 9. Figure 10 shows the CCI output current and voltage, which are nearly sinusoidal with respective total harmonic distortion (THD) values of 0.87% and 1.54%. From Figure 2, the maximum value of thepower coefficient occurred when the tip speed ratio reaches a value between 6 and 7. Equation (2) states that the tip speed ratioλ
is a function of the wind speed Uw and the mechanical angular velocity ωm of the turbine.Because the mechanical angular velocity of the turbine does not change immediately with the wind speed, λ deviates in the range of 6–7 with a subsequent spike of the power coefficient Cp. Then, the controller following the spike adjusts λ to the 6–7 range, and the power coefficient Cp returns to its maximum value. Figure 11(a) shows the PMSG output current and voltage on using a single-switch three-phase boost rectifier. The current THD value decreased from 11 to 2.57%. Figure11(b) shows the PMSG output current, voltage, and APF injected current on using an active filter. The current THD value decreased from 11 to 1.78%. Therefore, the advantage of using an APF over a single-switch three-phase boost rectifier is that it mitigates the current harmonics irrespective of the wind speed profile.

6. Conclusions

1) A new MPPT strategy is proposed to track maximum power from the wind turbine and to mitigate the PMSG output current harmonics using a single-switch threephase boost rectifier.
2) The single-switch three-phase boost rectifier being an active power factor correction technique corrects the power factor at the PMSG side to nearly unity.
3) The results show that the proposed MPPT strategy succeeded in tracking the maximum available power from the wind turbine irrespective of the wind speed profile.
4) The results show that the proposed LCL filter succeeded in harmonic mitigation at the inverter output currents and voltages.
5) The APF designed for harmonic mitigation at the PMSG output side was found to be better than the use of a single-switch three-phase boost rectifier irrespective of the wind speed variation.

7. Appendix

Wind turbine parameters:

Rated power 20 KW

Rated wind speed 12 m/sec

Cut in speed 3 m/sec

Turbine rotor radius 5 m

PMSG parameter :

d-Axis inductance 5.24 mH

q-Axis inductance 5.24 mH

Stator resistance 0.432Ω

Number of poles 36

Grid parameters:

d-Axis inductance 5.24 mH

q-Axis inductance 5.24 mH

Stator resistance 0.432 Ω

Number of poles 36

References

Johnson, G. L., Wind Energy Systems, Englewood Cliffs, NJ: Prentice-Hall, 2001.

Chen, H. L., "Overview of different wind generators and their comparisons," IET Renew. Power Generat., Vol. 2, pp. 123–138, 2008.

Nayar, C. V., Islam, S. M., Dehbonei, H., Tan, K., and Sharma, H., Power Electronics for Renewable Energy Sources, Lausanne, Switzerland: Elsevier Inc., chapter 27, pp. 673–716, 2007.

Koutroulis, E., and Kalaitzakis, K., "Design of a maximum power tracking system for wind energy conversion applications," IEEE Trans. Industrial Electron., Vol. 53, pp. 486–494, 2006.

De Broe, A. M., Drouilhet, S., and Gevorgian, V., "A peak power tracker for small wind turbines in battery charging applications," IEEE Trans. Energy Conversion, Vol. 14, No. 4,pp. 1630–1635, December 1999.

Goodfellow, D., Smith, G. A., and Gardner, G., Control Strategies for Variable Speed Wind Energy Recovery, Leicester, UK: University of Leicester, 1987.

Miller, A., Muljadi, E., and Zinger, D. S., "A variable speed wind turbine power control," IEEE Trans. Energy Conversion, Vol. 12, pp. 181–186, June 1997.

Thiringer, T., and Linders, J., "Control by variable rotor speed of a fixed-pitch wind turbine operating in a wide speed range," IEEE Trans. Energy Conversion, Vol. 8, pp. 520–526, 1993.

Haque, M. E., Muttaqi, K. M., and Negnevitsky, M., "Control of a stand alone variable speed wind turbine with a permanent magnet synchronous generator," IEEE Power and Energy Society General Meeting on Conversion and Delivery of Electrical Energy, pp. 1–8, Pittsburgh, PA, 20–24 July 2008.

Wang, Q., and Chang, L., "An intelligent maximum power extraction algorithm for inverterbased variable speed wind turbine systems," IEEE Trans. Power Electron., Vol. 19, pp. 1242–1249, 2004.

Li, H., Shi, K. L., and Mclaren, P. G., "Neural network based sensorless maximum wind energy capture with compensated power coefficient," IEEE Trans Industrial Appl., Vol. 41, pp. 1548–1556, 2005.

Amei, K., Takayasu, Y., Ohji, T., and Sakui, M., "A maximum power control of wind generator system using a permanent magnet synchronous generator and a boost chopper circuit," Power Conversion Conference (PCC), Vol. 3, pp. 1447–1452, Osaka, Japan, 2002.

Tan, K., and Islam, S., "Optimum control strategies in energy conversion of PMSG wind turbine system without mechanical sensors," IEEE Trans. Energy Conversion, Vol. 19, pp. 392–399,2004.
Tan, K., and Islam, S., "Optimum control strategies in energy conversion of PMSG wind turbine system without mechanical sensors," IEEE Trans. Energy Conversion, Vol. 19, pp. 392–399,2004.
Boldea, I., Variable Speed Generators, Bristol, PA: Taylor and Francis Group, LLC, 2006.
Prasad, A. R., Ziogas, P. D., and Manias, S., "An active power factor correction technique for three-phase diode rectifier," IEEE Trans. Power Electron., Vol. 6, pp. 83–92, 1991.
Borle, L. J., and Nayar, C. V., "ZACE current controlled power flow for AC-DC power converters," IEEE Trans. Power Electron., Vol. 10, pp. 725–732, 1995.
Bakery, D. M., Agelidisyz, V. G., and Nayar, C. V., "A new digital zero average current error control algorithm for inverters," Intl. J. Electron., Vol. 87, pp. 481–490, 2000.
Borle, L. J., and Nayar, C. V., "Ramptime current control," Applied Power Electronics Conference and Exposition (APEC '96), Vol. 2, pp. 828–834, San Jose, CA, 1996.
Borle, L. J., "A three-phase grid-connected inverter with improved ramptime current control inprogrammable logic," Power Electronic Drives and Energy Systems International Conference,Vol. 1, pp. 452–457, Perth, Australia, 1998.
Abdel-Salam, M., Ahmed, A., and Abdel-Sater, M., "Ramptime current-controlled APF for harmonic mitigation, power factor correction and load balancing," Proceedings of the 14th International Middle East Power System Conference (MEPCON'10), pp. 144–150, Cairo University, Cairo, Egypt, 19–21 December 2010.
Freris, L. L., Wind Energy Conversion Systems, Englewood Cliffs, NJ: Prentice-Hall, pp. 182–184, 1990.
Stensby, J. L., Phase-Locked Loops Theory and Applications, Boca Raton, FL: CRC PressLLC, 1997.
Liserre, M., Blaabjerg, F., and Hansen, S., "Design and control of an LCL-filter based threephase active rectifier," IEEE Trans. Industry Appl., Vol. 41, pp. 1281–1291, 2005.

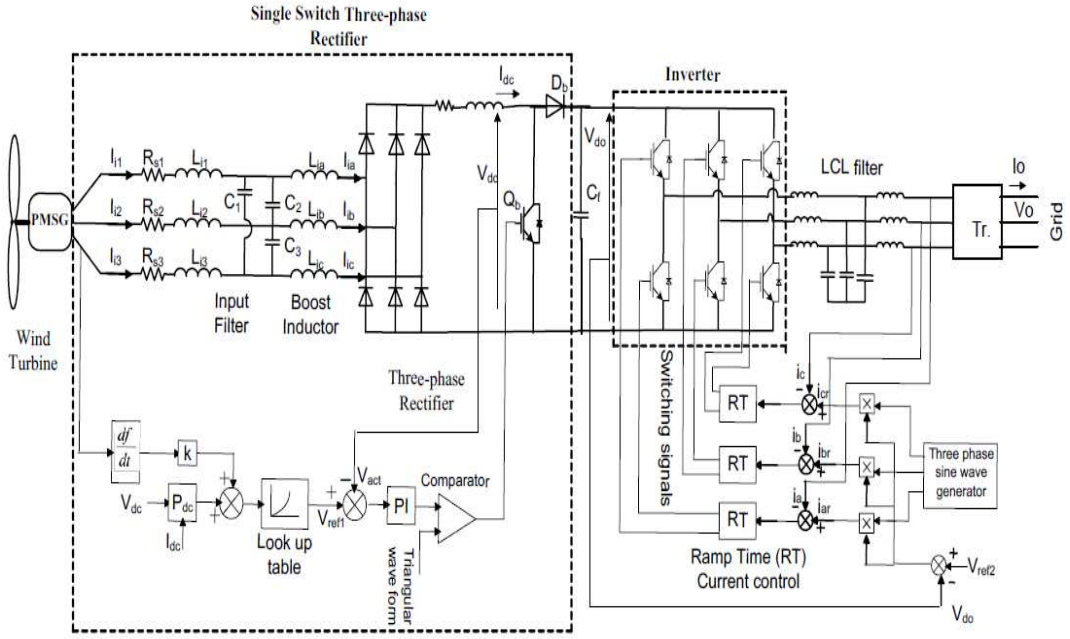

Figure 1. Proposed WECS

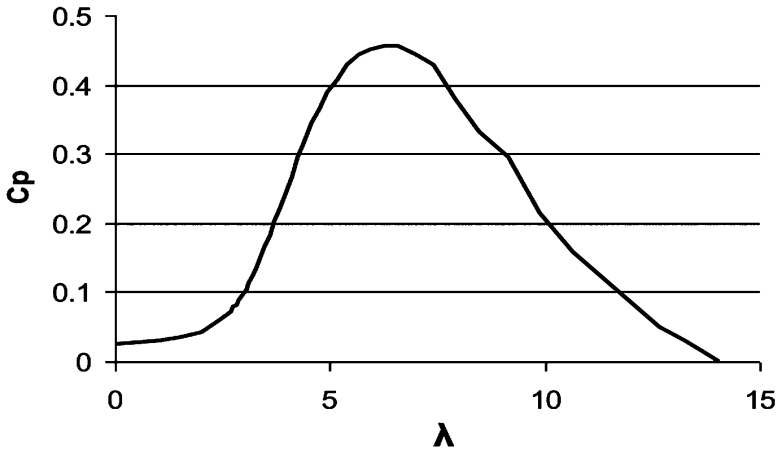

Figure 2. Power coefficient versus tip speed ratio

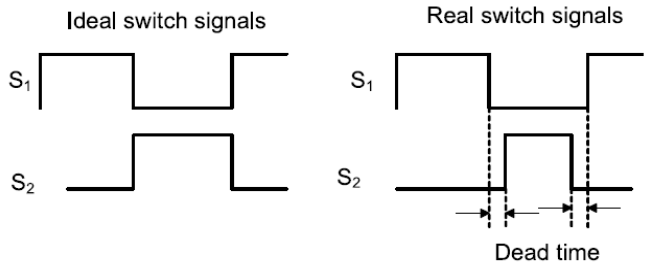

Figure 3. IGBT switch pulse with and without dead time

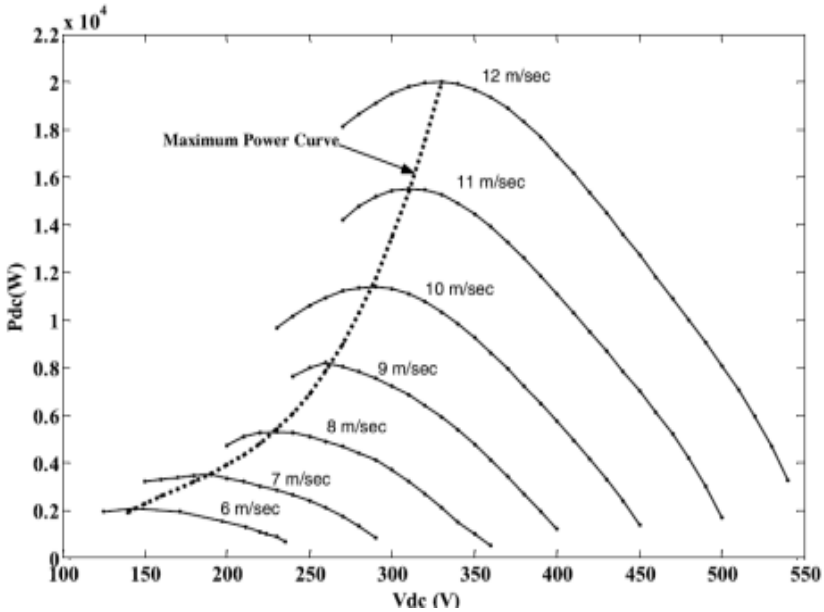

Figure 4. Generated DC power versus DC voltage of the WECS

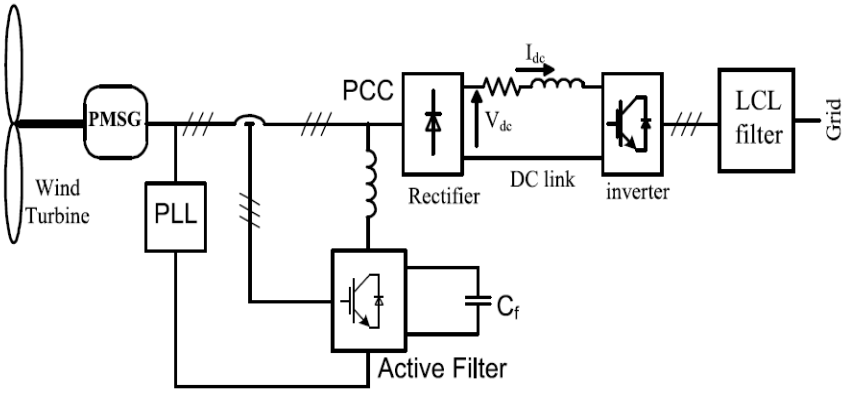

Figure 5. WECS with active power filter

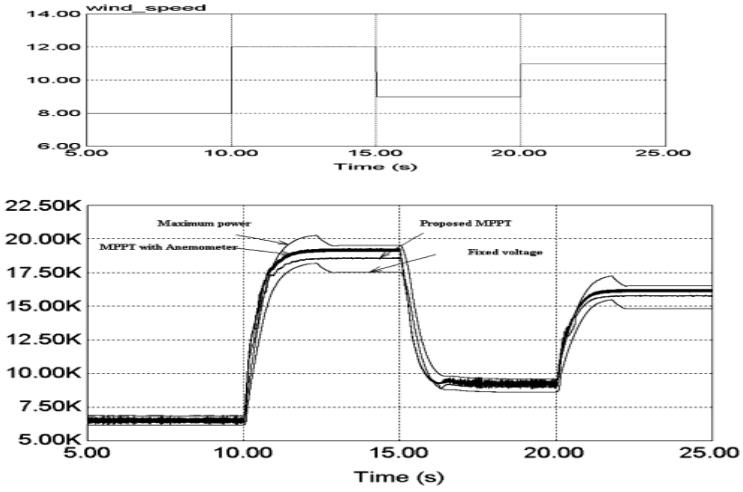

Figure 6. Wind speed (in m/sec) profile #1 and generated power (in kW) with different MPPT methods

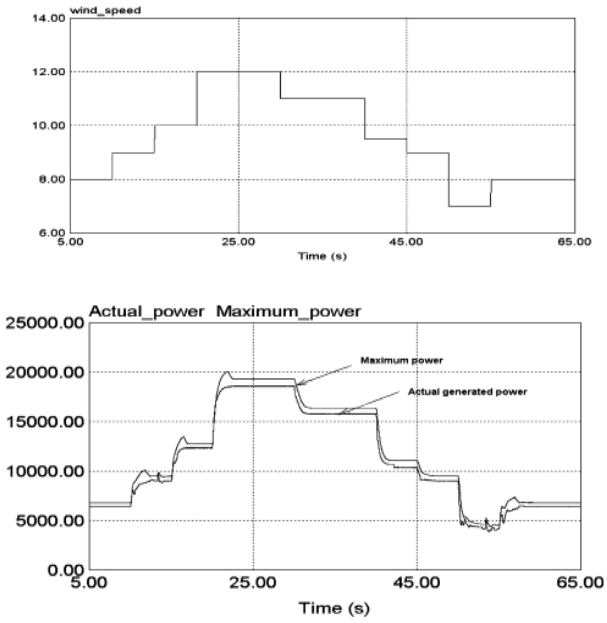

Figure 7. Wind speed (in m/sec) profile #2, maximum available power (in W), and the actual generated power

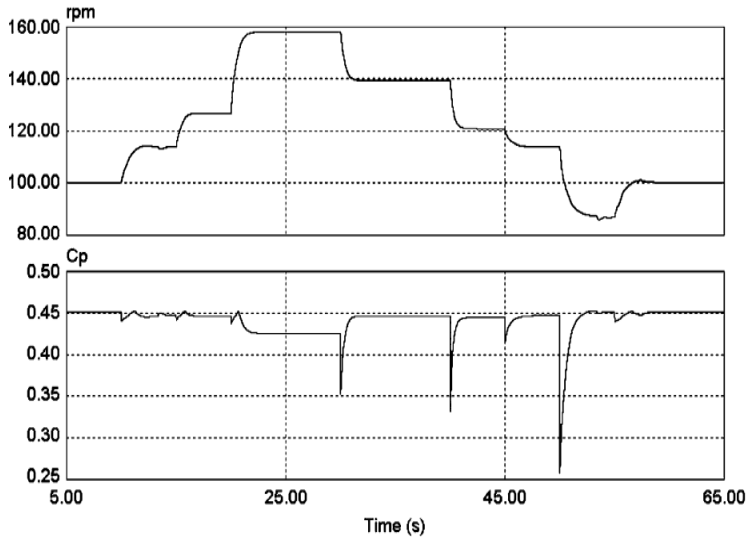

Figure 8. Power coefficient and shaft speed with wind profile #2

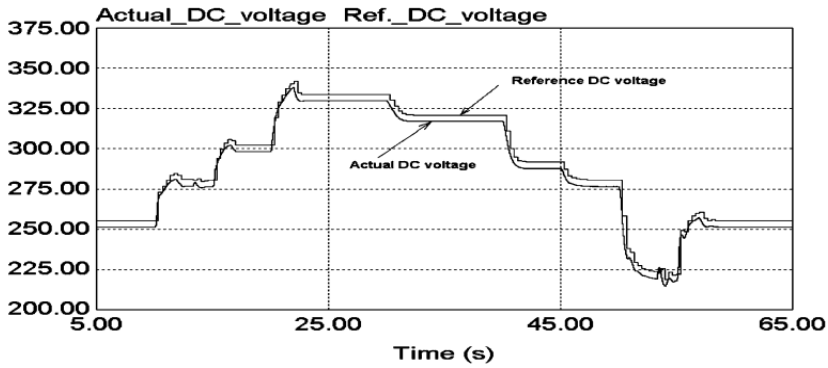

Figure 9. Reference DC voltage (in V) and actual DC voltage (in V) with wind profile #2.

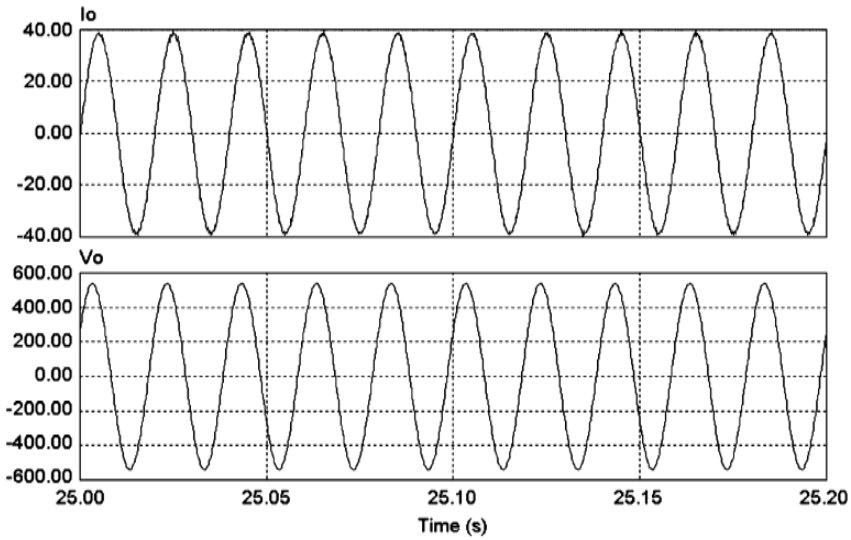

Figure 10. CCI output current (in A) and line-line voltage (in V) with wind profile #2

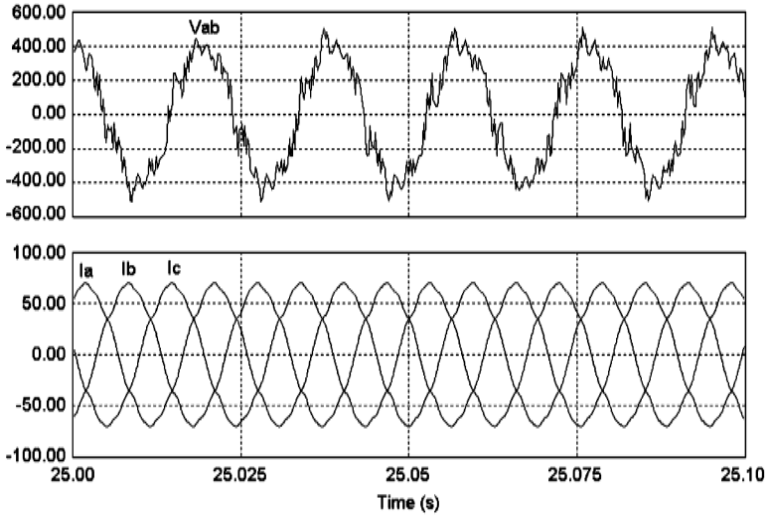

Figure 11. PMSG output current (in A) and line-line voltage (in V) with single-switch threephase boost rectifier for wind profile #2

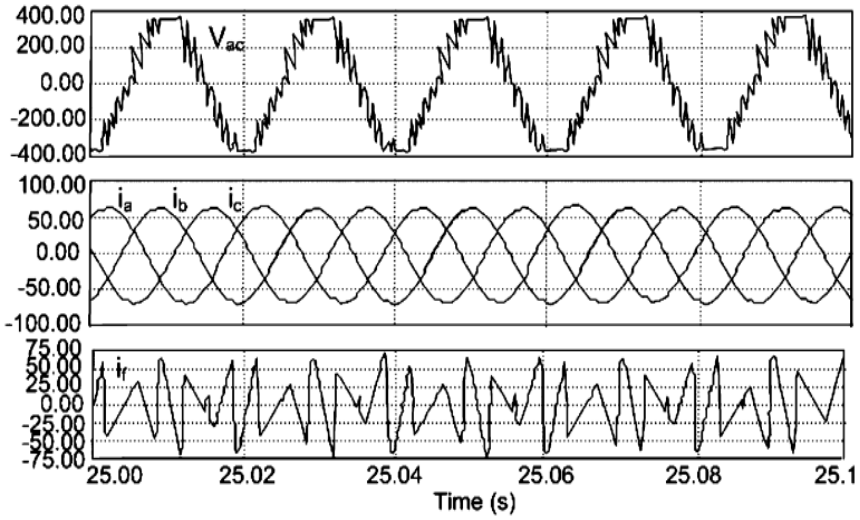

Figure 12. PMSG output current (in A), line-line voltage (in V) and injected current (in A) with active power filter for wind profile #2